CrystEngComm

Accepted Manuscript

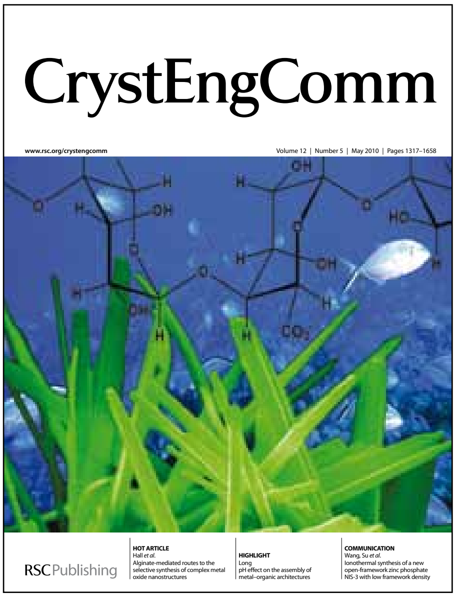

This is an *Accepted Manuscript*, which has been through the RSC Publishing peer review process and has been accepted for publication.

Accepted Manuscripts are published online shortly after acceptance, which is prior to technical editing, formatting and proof reading. This free service from RSC Publishing allows authors to make their results available to the community, in citable form, before publication of the edited article. This *Accepted Manuscript* will be replaced by the edited and formatted *Advance Article* as soon as this is available.

To cite this manuscript please use its permanent Digital Object Identifier (DOI®), which is identical for all formats of publication.

More information about *Accepted Manuscripts* can be found in the **Information for Authors**.

Please note that technical editing may introduce minor changes to the text and/or graphics contained in the manuscript submitted by the author(s) which may alter content, and that the standard **Terms & Conditions** and the **ethical guidelines** that apply to the journal are still applicable. In no event shall the RSC be held responsible for any errors or omissions in these *Accepted Manuscript* manuscripts or any consequences arising from the use of any information contained in them.

RSC Publishing

www.rsc.org/crystengcomm
Registered Charity Number 207890

Dynamic Article Links ▸

CrystEngComm

Cite this: DOI: 10.1039/c0xx00000x

www.rsc.org/crystengcomm

paper

Growth of aragonite phase calcium carbonate on the surface of titania-modified filter paper†

Tao Niu, Junbo Xu and Jianguo Huang*

Received (in XXX, XXX) Xth XXXXXXXXX 20XX, Accepted Xth XXXXXXXXX 20XX
DOI: 10.1039/b000000x

A new cellulose/aragonite composite material was fabricated by deposition of needle-like aragonite calcium carbonate crystals on the surface of ultrathin titania gel film modified filter paper. The titania-modified filter paper after preculeation with calcium carbonate nanoparticles was put in the classic geothermal water for the growth of the needle-like aragonite calcium carbonate crystals, and the needle-like calcium carbonate crystals were guaranteed to be pure aragonite. The mechanism of the formation of the pure aragonite crystals is that the calcium carbonate crystals may undergo a dissolution and recrystallization process. After the surface modification with monolayer of sodium stearate, this composite material was endowed with superhydrophobic property showing a water contact angle of 153°.

Introduction

Calcium carbonate is a well-known abundant biocompatible inorganic biomineral over the variety of functional inorganic crystals. It has been reported that calcium carbonate based composite materials possess significant potentials in various fields such as orthopedic implants,[1,2] drug delivery systems[3,4] and optical sensors.[5] Calcite which has the square shape is the most stable phase of calcium carbonate crystals. The metastable phase of calcium carbonate, aragonite, is unstable and may quickly transform to calcite when it forms. The aragonite crystals have special morphologies like rod or needle-shaped particles compared with the square shape calcite crystals, which have been employed as additives in the products of paper, plastic and rubber.[6–8] A number of attempts have been made to control the morphologies of the calcium carbonate crystals and to get high phase purity of which.[9–12] For examples, adding poly(acrylic acid) (PAA),[13–16] poly(ethylenimine) (PEI)[17] or poly(vinyl alcohol) (PVA)[18] to the crystal growth systems generate the metastable phases of calcium carbonate. It was reported that the employment of water-soluble terpolymers lead to the formation of calcium carbonate with unique morphologies.[19,20] The results showed that the functional groups like hydroxyl, carboxyl and amino in the polymers could interact with calcium ions to form complex compounds which restrained the transformation from metastable crystal phase to calcite. Besides the addition of polymer additives, the functionalization and supramolecular organization of 5-hexadecyloxyisophthalic acid made the nucleation of aragonite happen at the air/water interface.[21]

Magnesium ion has been proven to have important influence on the formation of aragonite crystals.[22–24] It may inhibit the nucleation and growth of calcite because of the difficulty in dehydration of magnesium ions.[25] And Mg^{2+} increases the solubility of calcite by subsitituing Ca^{2+} in calcite lattices.[26] As a result, with the presence of magnesium ions along with other additives, the formation of aragonite crystals became controllable. The classical geothermal water consisting of calcium, magnesium, sulfate and other ions was studied for the precipitation of aragonite phase calcium carbonate on the specimen surface.[27]

Natural cellulose substances with three-dimensional sophisticated hierarchical structure are adopted as ideal templates and scaffolds to fabricate novel functional artificial materials.[28–34] The combination of natural cellulose substances with inorganic crystals such as hydroxyapatite crystals,[35] calcium carbonate,[36–42] copper oxide,[43] zinc oxide[44–48] and cadmium selenide[28] crystals has driven much attention. The chemical reactions and interactions involved in the growth and deposition of the inorganic crystals on natural cellulose substances have been studied. Meanwhile, these composite materials have been proven to have potential applications in strain sensor,[44] antibacterium,[45,48] photocatalysis of rhodamine[46] and optical material.[28] As a result of the known superiority of the natural cellulose substances and the calcium carbonate crystals, designing

---

Department of Chemistry, Zhejiang University, Hangzhou, Zhejiang 310027, China. E-mail: jghuang@zju.edu.cn; Fax: +86-571-8795-1202

† Electronic supplementary information (ESI) available: SEM images and XRD patterns of paper/$(TiO_2)_5$/PAA/($CaCO_3$-x) samples; SEM image of quartz/$(TiO_2)_5$/($CaCO_3$-48) sample and the wettability results of the quartz/$(TiO_2)_5$/($CaCO_3$-48) sample after modification with sodium stearate. See DOI: 10.1039/b000000x/

cellulose/$CaCO_3$ composites has attracted much interest.[36–42] However, there are still difficulties in immobilizing aragonite crystals with high purity on cellulose substances ascribing to the instability of aragonite phase. Whether the microwave-assisted method,[36] hydrothermal method,[37,40] or the other solution-based methods[38,39,41,42] only got the single phase of calcite or the mixture of calcite and aragonite.

Calcium carbonate crystals which have specific morphologies have been used for fabricating the superhydrophobic surfaces that have a water contact angle of greater than 150°.[27,49] A cactuslike aragonite coating modified with sodium stearate was deposited on the surface of stainless steel inspired by fouling mineralization in the classical geothermal water. The fabricated composite material showed good superhydrophobic property.[27] The cellulose substances, such as filter paper, cotton, cloth, are known as hydrophilic materials. Various methods have been done to make cellulose substances have the astonishing superhydrophobic feature.[33,50–54] By simply coating the linerboard paper with the fatty acid modified precipitated calcium carbonate suspension, a superhydrophobic paper surface was generated.[50] In our previous works, a superhydrophobic cellulose material was made by self-assembly of long alkyl chain silane monolayer on the surface of titania-modified filter paper.[53] And reversible photo-responsive wettability was acquired by decorating the titania-modified filter paper with photo-sensitive azobenzene monolayer.[54] After etching the filter paper in alkaline solution and the deposition of titania gel films and fluorinated siloxane, the obtained cellulose material became an amphiphobic material with the inhibition of the adhesion of bacteria.[33]

The modification of cellulose substance like common commercial filter paper with nanometer-thick titania gel films through surface sol–gel process make the inert cellulose surface more chemically active for further surface modification.[55] In this work, we immobilized the needle-like aragonite crystals on the surface of titania-modified filter paper by prenucleation treatment and immersing in the classical geothermal water for 48 h at 50 °C. After assembly of low surface energetic substance like sodium stearate, the obtained bulk hybrid material shows superhydrophobic features (Scheme 1). The deposition of ultrathin titania gel films and the use of the geothermal water are proven to be the essential factors for the pure aragonite phase to form and grow. We introduce a facile and low-cost methodology to change the hydrophilic filter paper to bulk superhydrophobic material by depositing calcium carbonate crystals on the surface of the titania-modified filter paper, of which the crystal phase and the morphology of the calcium carbonate crystals have been simply controlled.

Experimental

Chemicals

Filter paper (quantitative ashless) was bought from Hangzhou Whatman-Xinhua Filter Paper Co., Ltd. (China). Titanium *n*-butoxide ($Ti(O^nBu)_4$, TBT) was bought from Sigma-Aldrich, and poly (acrylic acid) (PAA, 50 wt% solution in water) was purchased from J&K Chemicals. All the other chemicals were guaranteed reagents and were used without further purification. Milli-Q water (resistivity, 18.2 MΩ cm) was used in all the related cases.

Growth of calcium carbonate on the titania-modified filter paper

Five layers of ultrathin titania gel films were deposited onto each cellulose nanofibres of the filter paper by means of the surface sol–gel process according to our previous work, using $Ti(O^nBu)_4$ (100 mM) in 1 : 1 ethanol–toluene (v : v) as precursor solution (Scheme 1a).[55] The thickness of the 5-layer titania ultrathin films was approximate 2.5 nm. A piece of dried titania-modified filter paper was put in a glass beaker containing 50.0 mL of $CaCl_2$ solution (0.2 M, pH 9.90) and kept for half an hour at 80 °C to let sufficient Ca^{2+} adsorbing onto the fibres of the titania gel films decorated filter paper through the proton exchange between the positively charged Ca^{2+} and the hydroxyl groups in the titania gel films. Then the decorated filter paper was washed thoroughly by pure water and put into another beaker containing 50.0 mL of Na_2CO_3 solution (0.3 M, pH 11.50). At the same time, the above 50.0 mL of $CaCl_2$ solution was quickly added with fiercely stirring and kept for 5 min at 80 °C to make the titania-modified filter paper fibres covered with calcium carbonate nucleus (Scheme 1b). Then the sample was washed with water and dried in air. The final pH value of the supernate after the prenucleation process was measured to be 10.89. After the prenucleation process, the sample was put into a glass beaker containing 1.0 L of the classical geothermal water (pH 8.11) which consists of NaCl (3.641 g L^{-1}), Na_2SO_4 (0.113 g L^{-1}), $NaHCO_3$ (0.332 g L^{-1}), $MgCl_2{\cdot}6H_2O$ (0.328 g L^{-1}), $CaCl_2$ (0.284 g L^{-1}) and KCl (0.177 g L^{-1}), and kept for a certain period of time (6, 12, 24 and 48 hours) at 50 °C to complete the growth of calcium carbonate crystals. The pH values of the geothermal water was 8.30, 8.46, 8.45 and 8.44 after the 6, 12, 24 and 48-h calcium carbonate crystal growth processes, respectively. Eventually, $CaCO_3$ coated titania-modified filter paper was obtained, denoted as paper/$(TiO_2)_5$/ ($CaCO_3$-x) where x refers to the different hours for the growth of calcium carbonate crystals in the geothermal water (Scheme 1c). And then the sample was washed by pure water and dried in air.

As a control experiment, a monolayer of PAA was deposited on the 5-layer titania modified filter paper. After deposition of one layer of PAA,[56] the prenucleation, growth of aragonite were exactly the same as those of the titania-modified filter paper sample mentioned above. The final sample obtained was denoted as paper/$(TiO_2)_5$/PAA/($CaCO_3$-x) where x refers to the different hours for the growth of calcium carbonate crystals in the geothermal water.

Another control experiment was carried out using quartz plate as substrate for the growth of calcium carbonate crystals. Five layers of ultrathin titania gel films were deposited onto the surface of the quartz plate referring to the previous work.[57] Also the prenucleation, growth of aragonite processes were exactly the same as those of the titania-modified filter paper samples mentioned above, except the growth time of the calcium carbonate crystals was only 48 h. The final obtained sample was denoted as quartz/$(TiO_2)_5$/($CaCO_3$-48).

Surface modification with sodium stearate

The $CaCO_3$ coated titania-modified filter paper was immersed in 3.0 wt% sodium stearate solution for 30 min at 80 °C, followed by washed with pure water and dried at 80 °C for 10 min. The sodium stearate which is a common kind of low surface energy substances was self-assembled to form a monolayer onto the surface of the calcium carbonate crystals that grew on the surface of the titania-modified filter paper (Scheme 1d).

Characterizations

Specimens which were cut into 1.0×1.0 cm^2 rectangular sheets were used for FE-SEM examinations. FE-SEM micrographs were obtained on a CorlzeisD Utral 55 instrument working at an acceleration voltage of 5 kV, the specimens were sputtered with gold to increase conductivity. For transmission electron microscope examinations, the aragonite crystals were dispersed in ethanol after scraped from the surface of the paper/$(TiO_2)_5$/($CaCO_3$-48) sample and the resulting suspension was dropped onto carbon-coated copper grid followed by drying in air. TEM and HR-TEM micrographs were acquired on a Philip-FEI TECNAI G2 F30 S-TWIN apparatus at an acceleration voltage of 300 kV. X-ray diffraction (XRD) patterns was obtained by Rigaku UltimaIV using a CuKα (λ = 0.15405 nm) radiation source. Raman spectra were obtained using a Jobin Yvon LabRam HR UV Raman spectrometer operating at the excitation wavelength of 532 nm. The wettability of the $CaCO_3$ coated titania-modified filter paper and quartz plate after modification with sodium stearate was characterized by measuring the water contact angle (CA) utilizing a commercial contact angle meter (Powereach, JC2000C1, Shanghai, China) at ambient temperature using a water droplet of 5.0 µL.

Results and discussion

Characterizations of the $CaCO_3$ coated titania-modified filter paper

The 5-layer titania-modified filter paper samples after prenucleation treatment were immersed in the classic geothermal water for different hours to accomplish the growth of calcium carbonate crystals (Scheme 1). The obtained composite material maintains the morphology of the initial bulk filter paper (the insert photo in Fig. 1d). As shown in Fig. 1a, when the growth time was 6 h, there were both square-shaped calcite and needle-like aragonite crystals on the surface of the titania-modified filter paper. When the crystal growth time extended to 12 h, the amounts of the calcite crystals decreased and the need-like aragonite crystals became more (Fig. 1b).

The surfaces of the titania-modified filter papers were almost entirely covered with needle-like aragonite and the square calcite was barely found after the immersion time extending to 24 h and 48 h, and the aragonite crystals grew much larger after 48 h of crystal growth compared with the paper/$(TiO_2)_5$/($CaCO_3$-24) sample (Fig. 1c and 1d). As seen from the enlarged image of the aragonite crystals in Fig. 1e, the length of the needle-like aragonite crystals ranges from several to tens of micrometers. Fig. 1f is the cross-sectional view of the $CaCO_3$ coated titania-modified filter paper after immersing in the geothermal water for 48 h, from which the thickness of the calcium carbonate crystal coating is estimated to be 30 µm.

TEM micrograph of an isolated aragonite crystal scraped from the paper/$(TiO_2)_5$/($CaCO_3$-48) sample is shown in Fig. 2a. The width of the aragonite crystal is less than 1 µm which is in accordance with the SEM observation given in Fig. 1e. From the HR-TEM micrograph shown in Fig. 2b, the lattice spacing was measured to be 0.237 nm corresponding to the (112) lattice plane of aragonite crystal, which confirms the formation of aragonite phase crystals.

Fig. 3 gives the XRD patterns of the four composite materials that obtained by the growth of $CaCO_3$ crystals on the surface of the titania-modified filter paper in the classical geothermal water for 6 h, 12 h, 24 h and 48 h. The three peaks appearing at 15°, 16.5° and 23° are the characteristic peaks of the cellulose substance itself indexing to (101), (101) and (002) respectively in all the four spectra,[58] which show no change in all the four samples of the different hours for the growth of calcium carbonate crystals. In the spectra of paper/$(TiO_2)_5$/($CaCO_3$-6) and paper/$(TiO_2)_5$/($CaCO_3$-12) samples, except for the peaks of cellulose substance, only the characteristic diffraction peak of (104) of calcite at 29° was clear, which suggest that the main crystal phase was calcite and very few aragonite crystals formed within 24 hours. And the main peaks of aragonite at 26°, 27°, 46° and 48° indexing to (111), (021), (221) and (202) respectively became obvious in the spectra of the paper/$(TiO_2)_5$/($CaCO_3$-24) and paper/$(TiO_2)_5$/($CaCO_3$-48) samples, meanwhile the characteristic diffraction peak of calcite at 29° vanished. The results show that aragonite phase became dominant and the calcite crystals decreased until the $CaCO_3$ coating consists of pure aragonite crystals.

Fig. 4 shows the Raman spectra of the same four samples that used for XRD characterization. There were four main peaks of aragonite appeared in the Raman spectra, the peaks at 151 cm^{-1} and 206 cm^{-1} corresponding to lattice mode of CO_3^{2-}, the peak at 704 cm^{-1} due to in-plane bending of CO_3^{2-} and the peak at 1085 cm^{-1} corresponding to symmetric stretching of CO_3^{2-}.[59] In the spectrum of the paper/$(TiO_2)_5$/($CaCO_3$-6) sample, only the peak at 1085 cm^{-1} was clear. And with the increasement of the immersion time, the four typical Raman spectral lines of aragonite became stronger. The Raman spectra give the consistent results with the XRD patterns, which imply that the calcite phase was dominant at the beginning of the growth of $CaCO_3$ crystals, and with the extending of the growth time, a relatively high phase purity of aragonite coating was obtained at the experimental condition employed above.

Without the ultrathin titania gel films pre-deposited on the surface of the filter paper, the $CaCO_3$ coating on the surface of the blank filter paper was the mixture of calcite and aragonite crystals and the coverage of the calcium carbonate crystals was much lower. Undergoing the same prenucleation and crystal growth processes employing the blank filter paper as a control experiment, the obtained samples were denoted as paper/($CaCO_3$-x), where x refers to the different crystal growth hours. There were very few calcium carbonate crystals formed on the surface of the blank filter paper even after 48 h of crystal growth in the geothermal water, and clearly the calcite crystals existed in all the four samples (Fig. 5). The coverage of aragonite crystals on the surface of the blank filter paper was obviously much lower compared with the samples with pre-coated titania ultrathin films (Fig. 1). These results imply that the pre-modification with ultrathin titania gel films is necessary for the growth of high phase purity and coverage of aragonite crystals. The activated hydroxyl groups in the titania gel films captured more calcium ions because of the proton exchange between -OH and Ca^{2+},[35] and the resulting complex compounds formed on the surface of the aragonite crystals slowed down the speed of the transformation from aragonite to calcite and restrained the growth of calcite.[36,60]

It was reported that the carboxyl groups have the same or even stronger effects on the control of calcium carbonate crystals growth than the hydroxyl groups do.[13−16,42,60] The utilizing of PAA made the coverage of calcium carbonate crystals on the cellulose fibres much higer.[42] Here, another PAA layer was deposited on the surface of the titania-modified filter paper and the same processes of prenucleation and crystal growth were used to conduct a control experiment. The samples created were denoted as paper/$(TiO_2)_5$/PAA/($CaCO_3$-x), where x refers to the hours for calcium carbonate crystal to grow. As seen from Fig. S1, the coverage of calcium carbonate crystals was a bit larger than the ones that without the modification with ultrathin titania gel films (Fig. 5), however much lower than the ones with the modification of ultrathin titania gel films (Fig. 1). And there were still lots of calcite crystals on the surface of the sample even after 48 h of crystal growth (Fig. S1, ESI†). These observations are identical with the XRD patterns shown in Fig. S2. There were characteristic peaks of calcite at 29° in all the four spectra. Compared with the previous works, the addition of PAA indeed increased the coverage of calcium carbonate crystal on the surface of cellulose fibres, however the carboxyl groups of PAA are more compatible for the nucleation of calcite phase.[16,41,42,60] As a result, the employment of PAA led to the pure phase of calcite[42] or the mixture of different calcium carbonate crystal phases,[13,16] instead of the pure phase of aragonite in this work. The generation of high phase purity of aragonite crystals needs accurate control of the additives like the appropriate molecular weight of PEI[17] or the appropriate amounts of PVA.[18] Whereas, in our system, the 5-layer titania ultrathin films are enough for the formation of high phase purity of aragonite crystals.

Compared with the SEM images shown in Fig. 1, the calcium carbonate crystals on the surface of the titania-modified quartz plate were really rare (Fig. S3, ESI†). The three-dimensional sophisticated structure and the relatively high roughness of the filter paper supply plenty of sites for the adsorption of calcium ions, thus more calcium carbonate crystals immobilized on the surface of the titania-modified filter paper. Nevertheless, on the surface of the two-dimensional planar substances like quartz plate, even with the decoration of ultrathin titania gel films, calcium carbonate crystals are difficult to be immobilized.

Mechanism of the formation of pure aragonite on the surface of the titania-modified filter paper

The classical geothermal water used for the growth of calcium carbonate crystals contains the necessary ions like calcium ions and bicarbonate ions for the calcium carbonate crystals to form and grow. The ultrathin titania gel films pre-deposited on the surface of filter paper have the similar stable function for the aragonite phase crystals as the added magnesium ions in the geothermal water.[16,27,61,62] Because after the proton exchange between the -OH groups in the titania gel films and the Ca^{2+} ions in the geothermal water, the complex compounds generated on the surface of the decorated filter paper favour for the formation and growth of aragonite crystals. The formation and growth of aragonite and the disappearance of calcite may experience a dissolution and recrystallization process (Scheme 2). Calcite is the most stable phase of calcium carbonate, which quickly formed when the titania-modified filter paper was immersed in the geothermal water at 50 °C. With the extending of the crystal growth time, the formed calcite crystals dissolved and recrystallized gradually to the aragonite phase. This dissolution and recrystallization process almost completed after 24 h (Fig. 3) and the aragonite crystals grew larger with the increasement of the immersion time seen from the results of the above SEM characterizations (Fig. 1). Finally, through this dissolution and recrystallization process in the classic geothermal water, the calcium carbonate crystals grown on the surface of the titania-modified filter paper transformed to pure aragonite phase referring to the XRD results (Fig. 3).

Wettability of the $CaCO_3$ coated titania-modified filter paper

The wettability of the $CaCO_3$ coated titania-modified filter paper samples was evaluated by the measure of water contact angle. Without the surface modification with sodium stearate, the water drops were quickly absorbed into the $CaCO_3$ coated titania-modified filter paper samples because the $CaCO_3$ coating, titania gel films and filter paper are all hydrophilic. After the modification with a monolayer of sodium stearate, the hydrophilic surfaces of the $CaCO_3$ coated titania-modified filter paper samples became hydrophobic. As seen in Fig. 6, the samples of which crystal growth time did not reach to 48 h showed the smaller contact angle values around 145°. After the growth time of the calcium carbonate crystals extended to 48 hours, the paper/$(TiO_2)_5$/($CaCO_3$-48) sample with surface modification gave a contact angle value of water of 153° ± 1° which is greater than the superhydrophobic limitation (150°). However, the paper/($CaCO_3$-48) and the paper/$(TiO_2)_5$/PAA/($CaCO_3$-48) samples with the modification of sodium stearate only gave the contact angle values of water around 100°. The changes of the wettability are corresponding to the changes of the roughness provided by the needle-like aragonite crystals on the surface of the samples. As seen from the Fig. 1d, the largest roughness came from the paper/$(TiO_2)_5$/($CaCO_3$-48) sample. Hence, after the surface modification with sodium stearate, the sample was endowed with superhydrophobic feature. On the contrary, the mixture of calcite and aragonite crystals and the lower coverage of calcium carbonate crystals of the paper/($CaCO_3$-48) (Fig. 5d) and the paper/$(TiO_2)_5$/PAA/($CaCO_3$-48) (Fig. S2d, ESI†) samples with surface modification led to much lower contact angle values. And compared with the work by using linerboard paper and the fatty acid modified precipitated calcium carbonate suspension to fabricate superhydrophobic material,[31] the calcium carbonate crystals on the surface of the paper/$(TiO_2)_5$/($CaCO_3$-48) sample in this work had the uniform morphology and high phase purity, and the composite material introduced here had the better superhydrophobic property.

The quartz/$(TiO_2)_5$/($CaCO_3$-48) sample after the modification with sodium stearate gives the water contact angle value of only 40° (Fig. S3, ESI†). The surface roughness supplied by the $CaCO_3$ coating was much lower on the quartz/$(TiO_2)_5$/($CaCO_3$-48) sample. The needle-like aragonite crystal coating captures lots of air to reduce the water/air contact area which makes the contribution to the hydrophobicity. As a result, compared with the sophisticated porous structure of the filter paper samples, the two-dimensional planar structure of the quartz plate is a main defect. All the results of the crystal phase, morphology of calcium carbonate crystals and the water contact angle values imply the success of fabricating a bulk superhydrophobic composite material combining the unique morphology and physical properties from the initial natural cellulose substance and high phase purity of aragonite together.

Conclusions

In conclusion, a facile way of growing pure aragonite crystals on the surface of the titania-modified filter papers has been introduced to fabricate cellulose/$CaCO_3$ composite material. After the prenucleation treatment and immersing in the geothermal water, the surface of the titania-modified filter paper was fully covered with needle-like aragonite crystals. The pre-modification with ultrathin titania gel films has been proven to be necessary and essential for the formation and stabilization of the aragonite crystals. It shows that the $CaCO_3$ coating on the surface of the titania-modified filter paper may experience a dissolution and recrystallization process to become pure aragonite phase. This brand new cellulose/$CaCO_3$ composite material has a relatively high aragonite phase purity compared with the other previous works which were only calcite phase or the mixture of calcite and aragonite. With the unique morphology and physical properties inheriting from the filter paper and the self-assembly of a monolayer of low surface energetic sodium stearate, this cellulose/$CaCO_3$ composite material was endowed with superhydrophobic property with a water contact angle of 153°, which has a potential specific application in superhydrophobic materials. The needle shaped aragonite crystals are expected to show promising applications in biomedical fields, and the aragonite based composite materials were reported to be applied in the cleanup of contaminated water.[63] Moreover, the present work shows promising potentials for designing and fabrication of artificial biomaterials with the combination of natural cellulose substances and various functional substances.

Acknowledgements

This work was supported by the National Key Project on Basic Research of China (2009CB930104) and the National Natural Science Foundation of China (21173192, J1210042).

Notes and references

1 R. A. Ahmed, A. M. Fekry and R. A. Farghali, *Appl. Surf. Sci.*, 2013, **285P**, 309–316.
2 H.-D. Yu, Z.-Y. Zhang, K. Y. Win, J. Chan, S. H. Teoh and M.-Y. Han, *Chem. Commun.*, 2010, **46**, 6578–6580.
3 S. Chen, D. Zhao, F. Li, R.-X. Zhuo and S.-X. Cheng, *RSC Adv.*, 2012, **2**, 1820–1826.
4 Y. Svenskaya, B. Parakhonskiy, A. Haase, V. Atkin, E. Lukyanets, D. Gorin and R. Antolini, *Biophys. Chem.*, 2013, **182**, 11–15.
5 R. K. Pai and M. Cotlet, *J. Phys. Chem. C*, 2011, **115**, 1674–1681.
6 G. Li, Z. Li and H. Ma, *Int. J. Miner. Process.*, 2013, **123**, 25–31.
7 Z. Hu, M. Shao, Q. Cai, S. Ding, C. Zhong, X. Wei and Y. Deng, *J. Mater. Process. Technol.*, 2009, **209**, 1607–1611.
8 Z. Hu and Y. Deng, *Powder Technol.*, 2004, **140**, 10–16.
9 R. K. Pai, K. Jansson and N. Hedin, *Cryst. Growth Des.*, 2009, **9**, 4581–4583.
10 G.-T. Zhou, J. C. Yu, X.-C. Wang and L.-Z. Zhang, *New. J. Chem.*, 2004, **28**, 1027–1031.
11 D. Chakrabarty and S. Mahapatra, *J. Mater. Chem.*, 1999, **9**, 2953–2957.
12 Z. Huang and G. Zhang, *Cryst. Growth Des.*, 2012, **12**, 1816–1822.
13 Y. Pan, X. Zhao, Y. Sheng, C. Wang, Y. Deng, X. Ma, Y. Liu and Z. Wang, *Colloid Surf. A-Physicochem. Eng. Asp.*, 2007, **297**, 198–202.
14 H. Matahwa, V. Ramiah and R. Sanderson, *J. Cryst. Growth*, 2008, **310**, 4561–4569.
15 K. Naka, S.-C. Huang and Y. Chujo, *Langmuir*, 2006, **22**, 7760–7767.
16 A. Kotachi, T. Miura and H. Imai, *Cryst. Growth Des.*, 2006, **6**, 1636–1641.
17 H. K. Park, I. Lee and K. Kim, *Chem. Commun.*, 2004, 24–25.
18 I. W. Kim, R. E. Robertson and R. Zand, *Cryst. Growth Des.*, 2005, **5**, 513–522.
19 R. K. Pai, S. Hild, A. Ziegler and O. Marti, *Langmuir*, 2004, **20**, 3123–3128.
20 R. K. Pai and S. Pillai, *Cryst. Growth Des.*, 2007, **7**, 215–217.
21 A. L. Litvin, S. Valiyaveettil, D. I. Kaplan and S. Mann, *Adv. Mater.*, 1997, **9**, 124–127.
22 R. K. Pai and S. Pillai, *J. Am. Chem. Soc.*, 2008, **130**, 13074–13078.
23 D. Walsh and S. Mann, *Nature*, 1995, **377**, 320–323.
24 F. Zhu, T. Nishimura, T. Sakamoto, H. Tomono, H. Nada, Y. Okumura, H. Kikuchi and T. Kato, *Chem. Asian J.*, 2013, **8**, 3002–3009.
25 N. Wada, K. Yamashita and T. Umegaki, *J. Cryst. Growth*, 1995, **148**, 297–304.
26 K. J. Davis, P. M. Dove and J. J. De Yoreo, *Science*, 2000, **290**, 1134–1137.
27 G. G. Wang, L. Q. Zhu, H. C. Liu and W. P. Li, *Langmuir*, 2011, **27**, 12275–12279.
28 T. Niu, Y. Gu and J. Huang, *J. Mater. Chem.,* 2011, **21**, 651–656.
29 Y. Luo, X. Liu and J. Huang, *J. Nanosci. Nanotechnol.,* 2013, **13**, 582–588.
30 Y. Gu and J. Huang, *Mater. Res. Bull.,* 2013, **48**, 429–434.
31 X. Liu, Y. Zhang, T. Wu, and J. Huang, *Chem. Commun.,* 2012, **48**, 9992–9994.
32 W. Xiao, H. Hu, and J. Huang, *Sens. Actuators, B*, 2012, **171–172**, 878–885.
33 C. Jin, Y. Jiang, T. Niu and J. Huang, *J. Mater. Chem.,* 2012, **22**, 12562–12567.
34 W. Xiao and J. Huang, *Langmuir*, 2011, **27**, 12284–12288.
35 M. González, E. Hernández, J. A. Ascencio, F. Pacheco, S. Pacheco and R. Rodríguez, *J. Mater. Chem.,* 2003, **13**, 2948–2951.
36 M.-G. Ma, L.-H. Fu, R.-C. Sun and N. Jia, *Carbohydr. Polym.,* 2012, **90**, 309–315.
37 M.-G. Ma, L.-H. Fu, S.-M. Li, X.-M. Zhang, R.-C. Sun and Y.-D. Dai, *Carbohydr. Polym.,* 2012**, 88**, 1470–1475.
38 Z. Zheng, B. Huang, H. Ma, X. Zhang, M. Liu, Z. Liu, K. W. Wong and W. M. Lau, *Cryst. Growth Des.,* 2007, **7**, 1912–1917.
39 E. Dalas, P. G. Klepetsanis and P. G. Koutsoukos, *J. Colloid Interface Sci.,* 2000, **224**, 56–62.
40 N. Jia, S.-M. Li, M.-G. Ma, R.-C. Sun and J.-F. Zhu, *Carbohydr. Polym.,* 2012, **88**, 179–184.
41 C. Vilela, C. S. Freire, P. A. Marques, T. Trindade, C. P. Neto and P. Fardim, *Carbohydr. Polym.,* 2010, **79**, 1150–1156.
42 L. Liu, D. He, G.-S. Wang and S.-H. Yu, *Langmuir*, 2011, **27**, 7199–7206.
43 M.-G. Ma, S.-J. Qing, S.-M. Li, J.-F. Zhu, L.-H. Fu and R.-C. Sun, *Carbohydr. Polym.,* 2013, **91**, 162–168.
44 H. Gullapalli, V. S. M. Vemuru, A. Kumar, A. Botello-Mendez, R. Vajtai, M. Terrones, S. Nagarajaiah and P. M. Ajayan, *Small*, 2010, **6**, 1641–1646.
45 S. Anitha, B. Brabu, D. J. Thiruvadigal, C. Gopalakrishnan and T. S. Natarajan, *Carbohydr. Polym.* 2012, **87**, 1065–1072.

46 S. Ye, D. Zhang, H. Liu and J. Zhou, *J. Appl. Polym. Sci.,* 2011, **121**, 1757–1764.

47 A. J. Gimenez, J. M. Yáñez-Limón and J. M. Seminario, *J. Phys. Chem. C*, 2011, **115**, 828–287.

48 I. Perelshtein, G. Applerot, N. Perkas, E. Wehrschetz-Sigl, A. Hasmann, G. M. Guebitz and A. Gedanken, *ACS Appl. Mater. Interfaces*, 2009, **1**, 361–366.

49 G. Zhang, D. Wang, Z.-Z. Gu and H. Möhwald, *Langmuir*, 2005, **21**, 9143–9148.

50 Z. Hu, X. Zen, J. Gong and Y. Deng, *Colloid Surf. A-Physicochem. Eng. Asp.,* 2009, **351**, 65–70.

51 S. Li, S. Zhang and X. Wang, *Langmuir*, 2008, **24**, 5585–5590.

52 B. Balu, V. Breedveld and D. W. Hess, *Langmuir*, 2008, **24**, 4785–4790.

53 S. Li, Y. Wei and J. Huang, *Chem. Lett.,* 2010, **39**, 20–21.

54 C. Jin, R. Yan and J. Huang, *J. Mater. Chem.,* 2011, **21**, 17519–17525.

55 J. Huang and T. Kunitake, *J. Am. Chem. Soc.,* 2003, **125**, 11834–11835.

56 J. Huang and T. Kunitake, *J. Mater. Chem.* 2006, **16**, 4257–4264.

57 S.-W. Lee, I. Ichinose and T. Kunitake, *Langmuir* 1998, **14**, 2857–2863.

58 D. V. Parikh, D. P. Thibodeaux and B. Condon, *Text. Res. J.* 2007, **77**, 612–616.

59 Y. Ma, L. Qiao and Q. Feng, *Biol. Appl.,* 2012, **32**, 1963–1970.

60 R. Lakshminarayanan, S. Valiyaveettil and G. L. Loy, *Cryst. Growth Des.,* 2003, **3**, 953–958.

61 W. Xiao, J. Liu, Q. Chen, Y. Wu, L. Dai and T. Wu, *Cryst. Res. Technol.,* 2011, **46**, 1071–1078.

62 F. Zhang, X. Yang and F. Tian, *Mater. Sci. Eng. C-Mater. Biol. Appl.,* 2009, **29**, 2530–2538.

63 Y. Du, L. Zhu and G. Shan, *J. Colloid Interface Sci.*, 2012, **367**, 378–382.

Scheme/Figure Legends:

Scheme 1 Illustration of the fabrication process of the superhydrophobic aragonite phase $CaCO_3$ coated titania-modified filter paper.

Fig. 1. SEM micrographs of samples (a) paper/$(TiO_2)_5$/($CaCO_3$-6); (b) paper/$(TiO_2)_5$/($CaCO_3$-12); (c) paper/$(TiO_2)_5$/($CaCO_3$-24); (d) paper/ $(TiO_2)_5$/($CaCO_3$-48), the inset is a photo of the sample. (e) The enlarged SEM image of (d), (f) The cross-sectional SEM micrograph of sample paper/ $(TiO_2)_5$/($CaCO_3$-48).

Fig. 2 (a) TEM and (b) HR-TEM micrographs of the aragonite crystal that scraped from the surface of the paper/$(TiO_2)_5$/($CaCO_3$-48) sample.

Fig. 3 XRD patterns of samples (a) paper/$(TiO_2)_5$/($CaCO_3$-6), (b) paper/$(TiO_2)_5$/($CaCO_3$-12), (c) paper/$(TiO_2)_5$/($CaCO_3$-24), and (d) paper/$(TiO_2)_5$/($CaCO_3$-48).

Fig. 4 Raman spectra of samples (a) paper/$(TiO_2)_5$/($CaCO_3$-6), (b) paper/$(TiO_2)_5$/($CaCO_3$-12), (c) paper/$(TiO_2)_5$/($CaCO_3$-24), and (d) paper/ $(TiO_2)_5$/($CaCO_3$-48).

Fig. 5 SEM micrographs of samples (a) paper/($CaCO_3$-6), (b) paper/($CaCO_3$-12), (c) paper/($CaCO_3$-24), (d) paper/($CaCO_3$-48). (e–h) The enlarged images of (a–d) respectively. The arrows refer to the calcite crystals.

Scheme 2 The dissolution and recrystallization process of the formation and growth of aragonite crystals.

Fig. 6 Water droplet pictures on the surfaces of samples (a) paper/$(TiO_2)_5$/($CaCO_3$-6), (b) paper/$(TiO_2)_5$/($CaCO_3$-12), (c) paper/ $(TiO_2)_5$/($CaCO_3$-24), and (d) paper/$(TiO_2)_5$/($CaCO_3$-48) after modification with sodium stearate.

Growth of aragonite phase calcium carbonate on the surface of titania-modified filter paper

Tao Niu, Junbo Xu and Jianguo Huang*

Department of Chemistry, Zhejiang University, Hangzhou, Zhejiang 310027, China

E-mail: jghuang@zju.edu.cn

Graphic Abstract Entry:

Growth of aragonite phase calcium carbonate on the surface of titania-modified filter paper

Tao Niu, Junbo Xu and Jianguo Huang*

Growth of aragonite $CaCO_3$ crystals on titania coated cellulose fibres of filter paper was achieved to give a superhydrophobic composite.

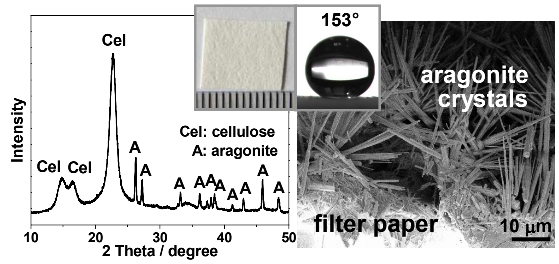

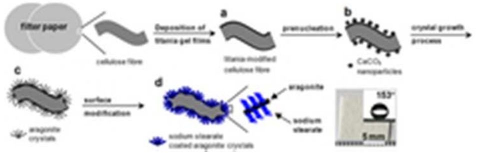

Illustration of the fabrication process of the superhydrophobic aragonite phase $CaCO_3$ coated titania-modified filter paper.
9x3mm (600 x 600 DPI)

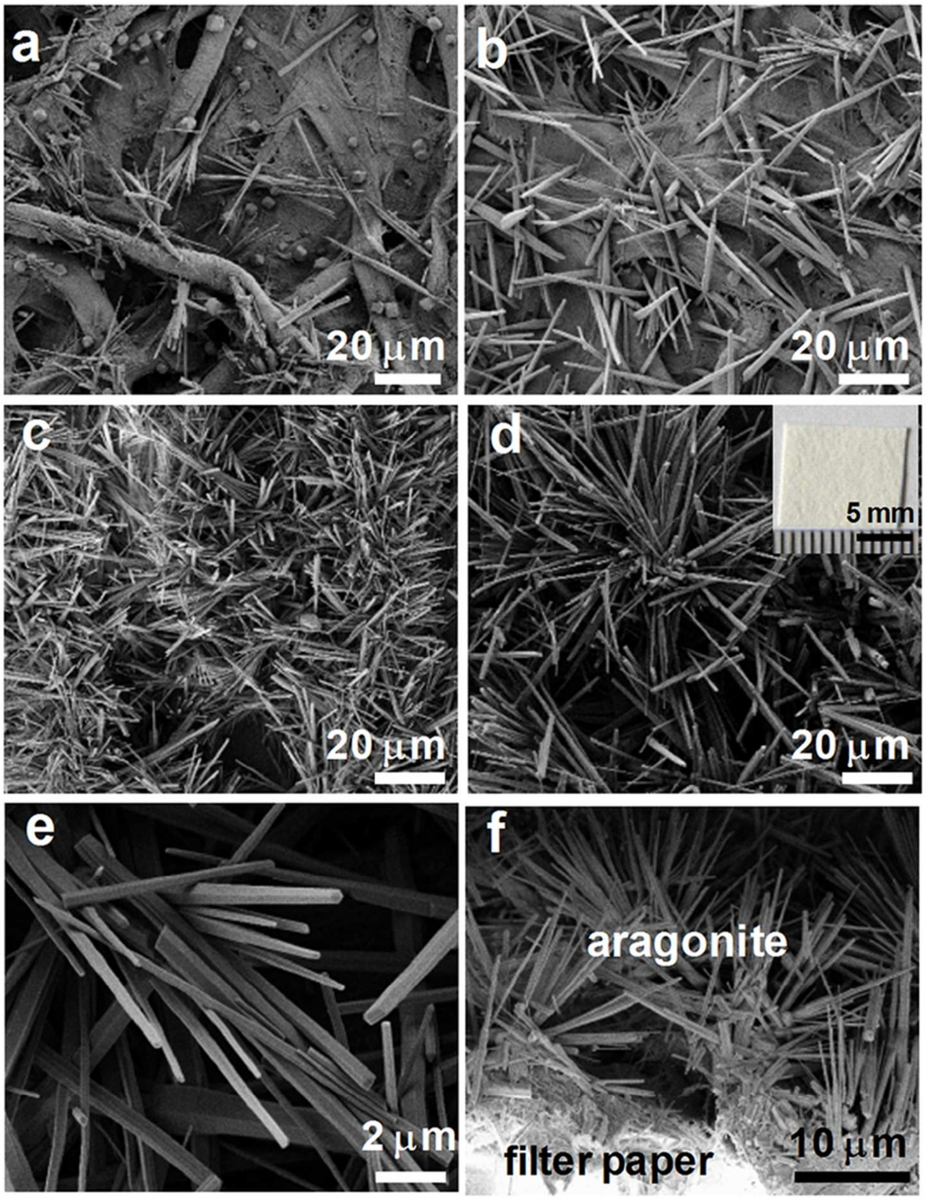

SEM micrographs of samples (a) paper/(TiO_2)$_5$/($CaCO_3$-6); (b) paper/(TiO_2)$_5$/($CaCO_3$-12); (c) paper/(TiO_2)$_5$/($CaCO_3$-24); (d) paper/ (TiO_2)$_5$/($CaCO_3$-48), the inset is a photo of the sample. (e) The enlarged SEM image of (d), (f) The cross-sectional SEM micrograph of sample paper/(TiO_2)$_5$/($CaCO_3$-48).
32x42mm (600 x 600 DPI)

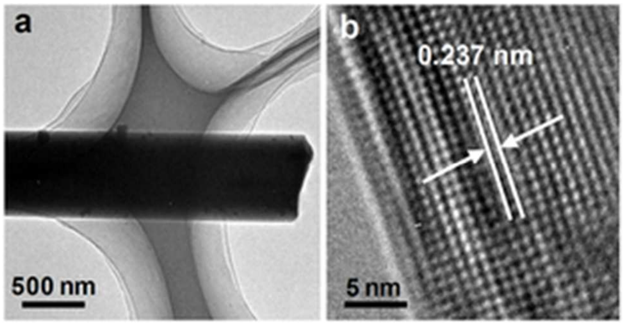

(a) TEM and (b) HR-TEM micrographs of the aragonite crystal that scraped from the surface of the paper/$(TiO_2)_5$/($CaCO_3$-48) sample.
13x6mm (600 x 600 DPI)

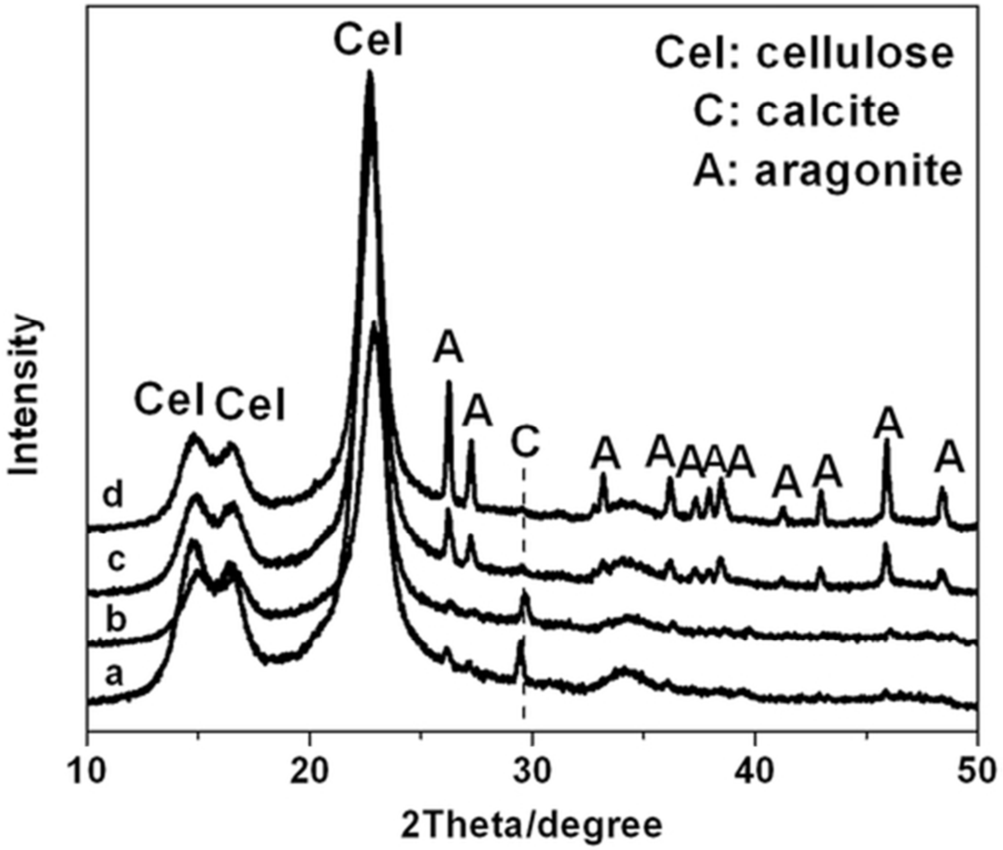

XRD patterns of samples (a) paper/$(TiO_2)_5$/($CaCO_3$-6), (b) paper/$(TiO_2)_5$/($CaCO_3$-12), (c) paper/$(TiO_2)_5$/($CaCO_3$-24), and (d) paper/$(TiO_2)_5$/($CaCO_3$-48).
21x18mm (600 x 600 DPI)

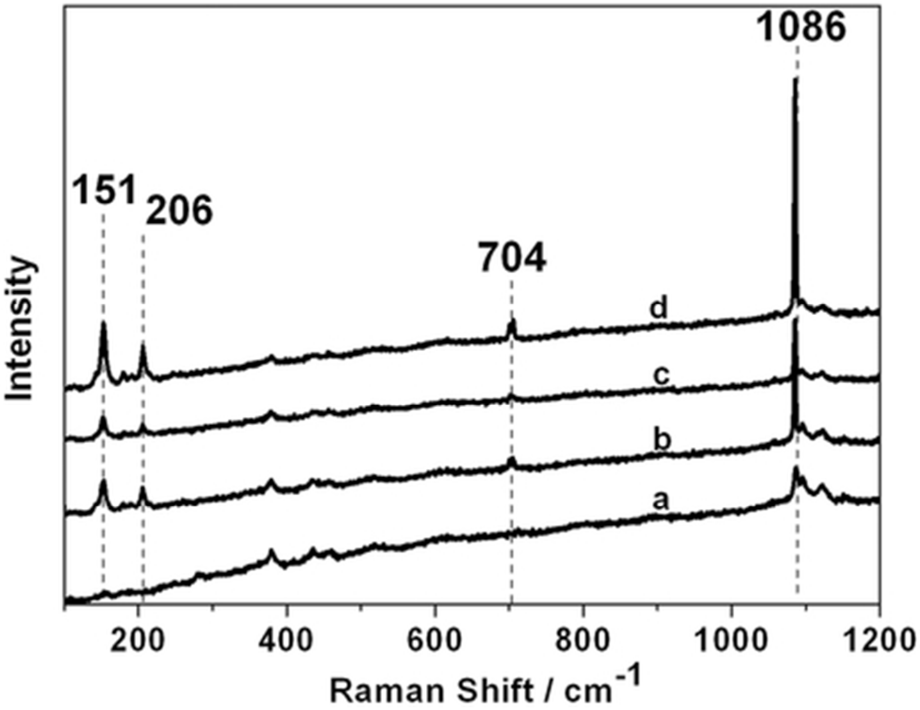

Raman spectra of samples (a) paper/$(TiO_2)_5$/($CaCO_3$-6), (b) paper/$(TiO_2)_5$/($CaCO_3$-12), (c) paper/$(TiO_2)_5$/($CaCO_3$-24), and (d) paper/ $(TiO_2)_5$/($CaCO_3$-48).
19x14mm (600 x 600 DPI)

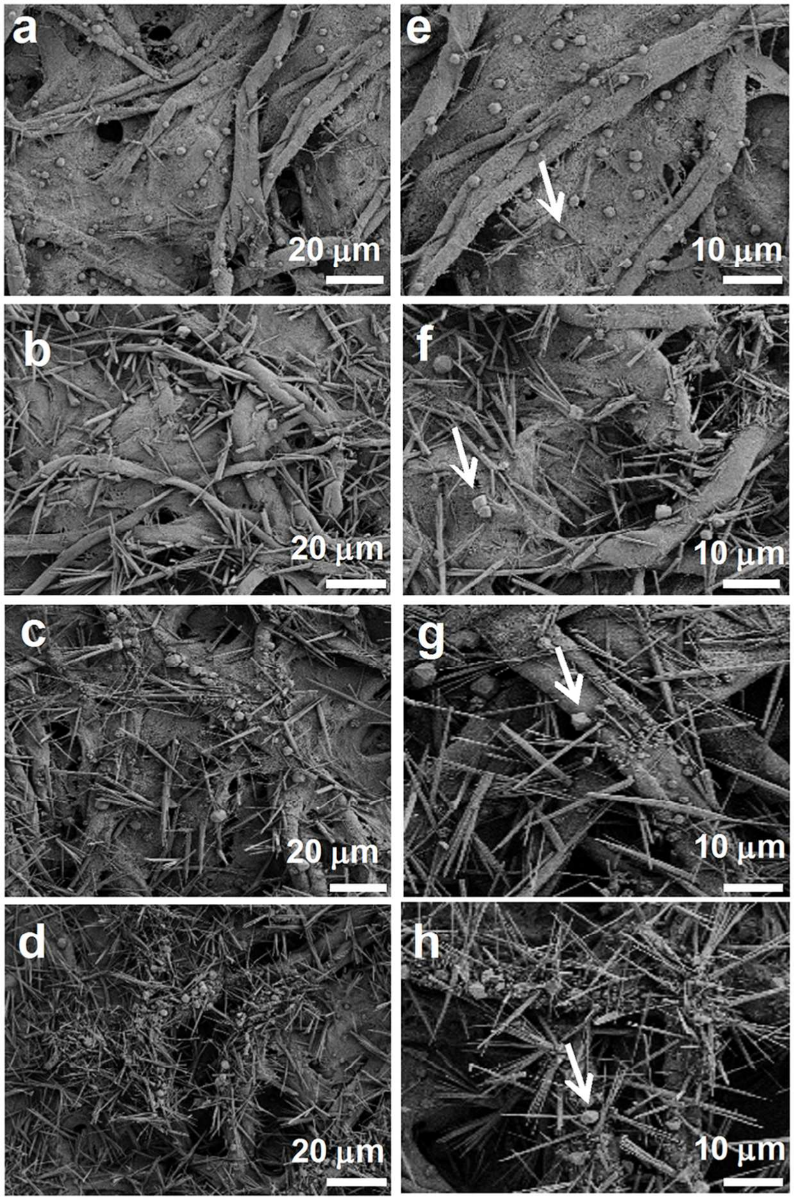

SEM micrographs of samples (a) paper/($CaCO_3$-6), (b) paper/($CaCO_3$-12), (c) paper/($CaCO_3$-24), (d) paper/($CaCO_3$-48). (e−h) The enlarged images of (a−d) respectively. The arrows refer to the calcite crystals.
41x63mm (600 x 600 DPI)

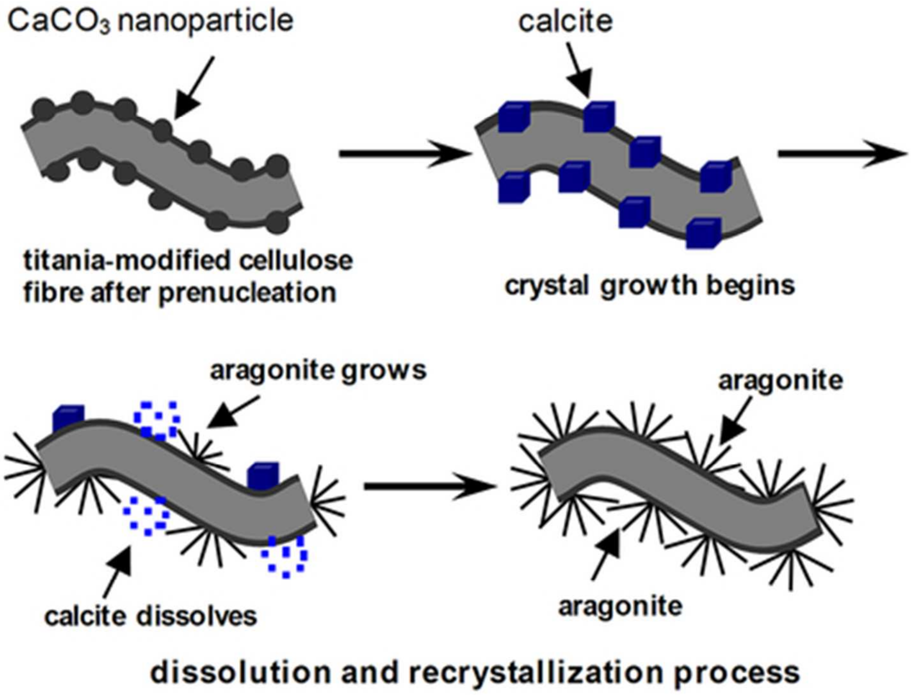

The dissolution and recrystallization process of the formation and growth of aragonite crystals.
19x14mm (600 x 600 DPI)

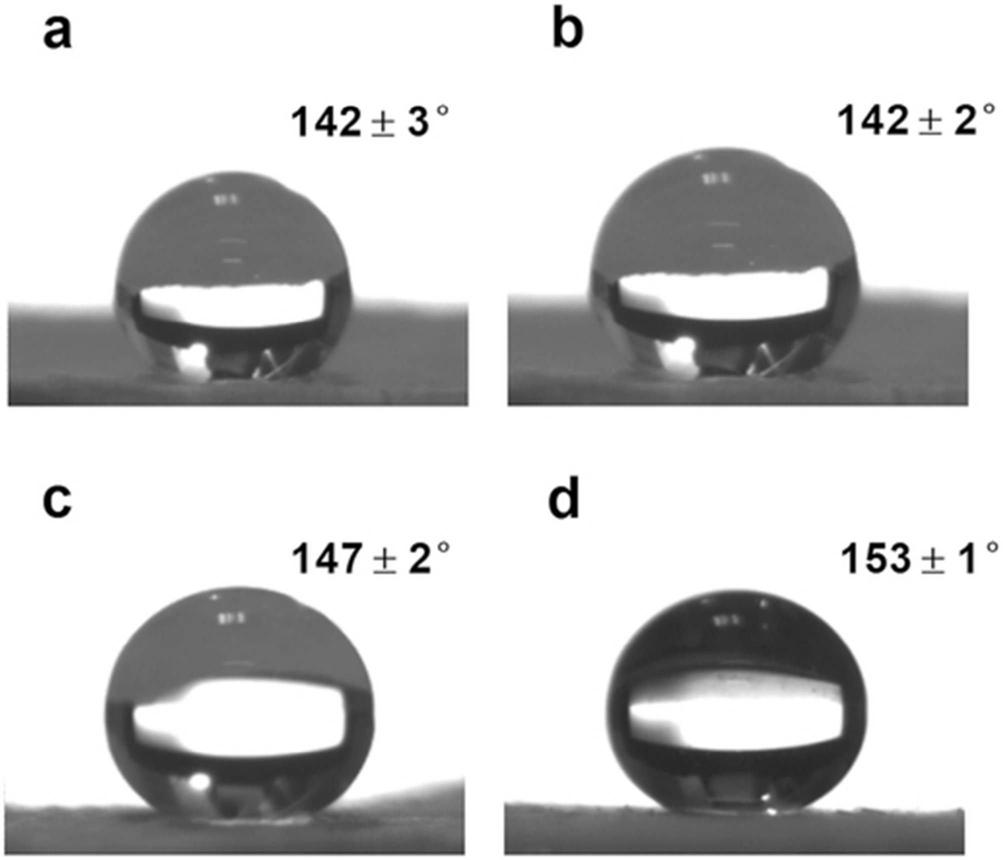

Water droplet pictures on the surfaces of samples (a) paper/$(TiO_2)_5$/($CaCO_3$-6), (b) paper/$(TiO_2)_5$/($CaCO_3$-12), (c) paper/$(TiO_2)_5$/($CaCO_3$-24), and (d) paper/$(TiO_2)_5$/($CaCO_3$-48) after modifica-tion with sodium stearate.
21x18mm (600 x 600 DPI)